AN ANALYSIS OF THE ACTIVE LAYER DEPTH IN BIOFILM-NUTRIENT DYNAMICS

NAREN VOHRA

1. Introduction

The purpose of this article is to analyse the role of the active layer depth in the biofilm-nutrient model. We consider a simple one dimensional system modeling a single microbial species which is growing by nutrient consumption. The microbial species occupies the biofilm region which is separated by an interface from the bulk-liquid region which has a high nutrient concentration. The nutrient also diffuses across the interface in a region called the active layer depth, which is where most of the biofilm growth activity takes place; as the biofilm grows, the interface moves and the species push into the bulk-liquid region.

Microbes play an important role in almost every material system. To model their growth, the two important components are the movement of the species and the consumption of the nutrient, or substrate, on which they thrive. The biofilm region typically consists of microbial cells, inert biomass, and extracellular polymeric substances (EPS), which is a gel-like polymeric substance produced by the microbial cells [7, 4, 6]. There exists an extensive amount of work that offers various models dealing with the growth and competition between multiple microbial species [1]. However, in this article we restrict ourselves to studying the growth of a single species with a single substrate. We also do not assume any decay of the biofilm though that is typically incorporated in the equation governing the growth of the biofilm.

Although the model that describes the biofilm-nutrient dynamics is a **non-stationary** one, most authors [4, 1] consider a **stationary** approximation. This approximation proves to be reasonable owing to the scale at which the biofilm is observed, which is around $[1, 100][\mu\text{m}]$ [1]. Further, this size warrants the use of a linear growth function rather than the well used non-linear Monod expression; an advantage of the linear function is that it even provides the stationary system with analytical solutions. Though this does greatly simplify the system, the errors vary greatly with the rest of the parameters. Moreover, some authors [4] even consider a semi-infinite biofilm domain, but we stick to the finite realm.

Biofilm-nutrient dynamics have been studied for a very long time. The distribution of the nutrient concentration throughout the domain plays an important role in determining the active layer depth. Some of these models have survived for more than a century [3] and are included in our analysis. In this article we primarily study the biofilm-nutrient model, the velocity of the interface separating the biofilm and the bulk liquid region and its relation to the active layer depth.

The outline of this article is as follows. In Sec. 2 we discuss the equations governing the biofilm-nutrient dynamics and give the distinction between the **non-stationary** and the **stationary** model. Sec. 3 deals with the numerical scheme used to solve system and in Sec. 4 we discuss the concept of the active layer depth and its different definitions. The analytical

solutions to the stationary problem are provided and discussed in Sec. 5. Finally, Sec. 6 deals with the velocity of the interface separating the biofilm and the bulk-liquid region and we conclude by quantifying the error between the non-stationary and the stationary system in Sec. 7.

2. Biofilm-Nutrient Model

Consider a region of length L ([m]) $\Omega = (0, L) \subset \mathbb{R}$ comprising of the biofilm region $\Omega_b = (0, \gamma)$ and the bulk-liquid region $\Omega_l = (\gamma, L)$, where $\gamma \equiv \gamma(t)$ ([m]) is the interface separating the biofilm and the bulk-liquid region. The equation governing the nutrient concentration, $N(x, t)$ ([kg/m^3]), is

$$N_t - \nabla((d_{N,b}\chi_{(0,\gamma)} + d_{N,w}\chi_{(\gamma,L)})\nabla N) = -\chi_{(0,\gamma)}m(N) \text{ in } \Omega. \tag{2.1a}$$

Here $d_{N,b}$ and $d_{N,w}$ ([m^2/s]) are the diffusivities of N in Ω_b and Ω_l, respectively, and m is the uptake rate which describes how fast the nutrient concentration is used by the biofilm. The biofilm is assumed to consist of a single species and its concentration is constant 1[kg/m^3] throughout Ω_b. To account for the growth of the biofilm, the velocity inside the biofilm, $v(x, t)$ ([m/s]), satisfies the conservation law

$$\nabla \cdot v = g(N) \text{ in } \Omega_b, \tag{2.1b}$$

where g is the growth rate of the biofilm. The velocity in turn depends on a growth potential, $\pi(x, t)$, as

$$v = -\lambda\nabla\pi \text{ in } \Omega_b, \tag{2.1c}$$

where the constant $\lambda = 1$. Finally, to accommodate the growing biofilm, the interface $\gamma = \partial\Omega_b \cap \partial\Omega_l$ moves and satisfies the equation

$$\frac{d\gamma}{dt} = v|_{x=\gamma}. \tag{2.1d}$$

The above system is completed with the following set of boundary conditions:

$$\nabla N|_{x=0} = 0, \ N(L, t) = N_{bd}. \tag{2.1e}$$

Equation (2.1e) consist of the impermeable boundary condition at $x = 0$ and the Dirichlet boundary condition at $x = L$. For the growth potential, the boundary conditions are

$$\nabla\pi|_{x=0} = 0, \ \pi|_{x=\gamma} = 0. \tag{2.1f}$$

As with N, an impermeable boundary condition is placed on π at $x = 0$ in (2.1f) along with a Dirichlet value at $x = \gamma$.

The uptake rate is given by the well known Monod function

$$m(N) = \frac{\kappa N}{k_N + N}, \tag{2.2}$$

where the constant k_N ([kg/m^3]) is called the Monod half-life and κ ([1/s]) is the specific substrate uptake rate. The growth rate g considered in this article is given by

$$g(N) = \kappa_B m(N), \tag{2.3}$$

where κ_B is a constant incorporating the maximum uptake rate and some yield coefficient.

The Monod expression (2.2) can be approximated by a constant or a linear function depending on the ration $\frac{k_N}{N}$:

$$\frac{k_N}{N} << 1 \implies m(N) \approx \kappa \tag{2.4a}$$

$$1 << \frac{k_N}{N} \implies m(N) \approx \frac{\kappa}{k_N} N. \tag{2.4b}$$

These two approximations are studied in more detail in the subsequent sections.

The system (2.1) above describes the non-stationary uptake of the nutrient concentration and the biofilm growth. Depending on the values of the parameters used, the system can be approximated well by its stationary counterpart i.e. the equation (2.1a) can be replaced by

$$-\nabla((d_{N,b}\chi_{(0,\gamma)} + d_{N,w}\chi_{(\gamma,L)})\nabla N) = -\chi_{(0,\gamma)} m(N) \text{ in } \Omega. \tag{2.5}$$

To further study the effect of the diffusivities $d_{N,b}$ and $d_{N,w}$, (2.5) is rewritten as

$$-\nabla((R_{N,bw}\chi_{(0,\gamma)} + 1\chi_{(\gamma,L)})\nabla N) = -\chi_{(0,\gamma)} \frac{m(N)}{d_{N,w}} \text{ in } \Omega, \tag{2.6}$$

with $R_{N,bw} = \frac{d_{N,b}}{d_{N,w}}$. The stationary system is complete with the same boundary conditions as in the non-stationary case.

3. Numerical Method

Spatial Discretisation. To compute the numerical solution to the non-stationary system (2.1a), we employ a cell-centered finite difference scheme with a staggered grid. The two subsets Ω_b and Ω_l of domain $\Omega = (0, L)$ are covered with $n_x = 100$ cells each, with x_i being the center of each cell denoted by $[x_{i-\frac{1}{2}}, x_{i+\frac{1}{2}}]$, $1 \le i \le 2n_x$.

Time Discretisation. We use implicit time stepping with time steps $t_n = n\tau$, where $\tau \approx O(10)$[s] is the uniform time step.

The approximate solution to the nutrient concentration, the growth potential, and the velocity is denoted by $N_i^n \approx N(x_i, t_n), \pi_i^n \approx \pi(x_i, t_n)$ and $v_i^n \approx v(x_{i-\frac{1}{2}}, t_n)$, respectively. The approximation to the interface is denoted by $\gamma^n \approx \gamma(t_n)$. Adopting the vector notation $N^n = [N_1^n N_2^n \dots N_{2n_x}^n]^T, \pi = [\pi_1^n \pi_2^n \dots \pi_{2n_x}^n]^T$, and $v = [v_1^n v_2^n \dots v_{2n_x+1}^n]^T$, the numerical scheme can we written as

$$\frac{N^n - N^{n-1}}{\tau} + \Delta_h \begin{bmatrix} d_{N,b} I_{n_x} & 0 \\ 0 & d_{N,w} I_{n_x} \end{bmatrix} N^n = -\begin{bmatrix} I_{n_x} & 0 \\ 0 & 0 \end{bmatrix} m(N^n), \tag{3.1}$$

$$\Delta_h \pi^n = g([N_1^n N_2^n \dots N_x^n]^T) \tag{3.2}$$

$$v^n = \nabla_h \pi^n \tag{3.3}$$

$$\frac{\gamma^{n+1} - \gamma^n}{\tau} = v_{n_x+1}^n, \tag{3.4}$$

where I_{n_x} is the $n_x \times n_x$ identity matrix, Δ_h and ∇_h are the discrete Laplacian (2nd order) and gradient (1st order) operators, respectively. The initial condition on N is taken as

$$N_i^0 = N_{bd}, \ \forall\ 1 \le i \le 2n_x, \ \gamma^0 = \frac{L}{2} \tag{3.5}$$

Newton's method was used to compute the solution of (3.1): Given N^{n-1}

Parameter	Value
n_x	100
τ	10.8 [s]
ϵ	1×10^{-8}
$i_{\max}$	30

TABLE 1. Values used in the numerical scheme in Sec. 3

while $(|\,\delta_N\,| > \epsilon)$ or $(i < i_{\max})$ **do**

$$R(N^n) = [R_1(N^n)R_2(N^n)\dots R_{2n_x}(N^n)]^T = \frac{N^n - N^{n-1}}{\tau} - \Delta_h \begin{bmatrix} d_{N,b}I_{n_x} & 0 \\ 0 & d_{N,w}I_{n_x} \end{bmatrix} + \begin{bmatrix} I_{n_x} & 0 \\ 0 & 0 \end{bmatrix} m(N^n)$$

$$J = \begin{bmatrix} \frac{\partial R_1}{\partial N_1^n} & \frac{\partial R_1}{\partial N_2^n} & \cdots & \frac{\partial R_1}{\partial N_{2n_x}^n} \\ \frac{\partial R_2}{\partial N_1^n} & \frac{\partial R_2}{\partial N_2^n} & \cdots & \frac{\partial R_2}{\partial N_{2n_x}^n} \\ \vdots & \vdots & \cdots & \vdots \\ \frac{\partial R_{2n_x}}{\partial N_1^n} & \frac{\partial R_{2n_x}}{\partial N_2^n} & \cdots & \frac{\partial R_{2n_x}}{\partial N_{2n_x}^n} \end{bmatrix}$$

$$\begin{aligned} \delta_N &= -J^{-1}R \\ N^n &\to N^n + \delta_N \\ i &= i + 1 \end{aligned}$$

end while

where ϵ is a fixed tolerance and $i_{\max}$ is the maximum number of iterations that are performed for each time step.

At the $(n+1)^{th}$ time step, since the interface, γ^{n+1}, changes, we regrid the domain Ω keeping the number of cells n_x in Ω_b and Ω_l fixed. Then, before solving for N^{n+1} in (3.1) we perform a linear interpolation to compute the values N^n at the new grid points.

The numerical scheme was solved using MATLAB. The values of the parameters used in the code are given in Tab. 1. The implementation of the numerical scheme was only marred by standard difficulties. Theory about the basic techniques and their implementation can be found in [5].

4. Active Layer Depth

The active layer, $\Omega_a \equiv \Omega_a(t) \subset \Omega_b$, is defined as the region in the biofilm domain Ω_b where the nutrient concentration N is high enough for there to be active metabolism. One quantity we are interested in is the depth $|\,\Omega_a\,|$ of the active layer and how it depends on the various parameters used. There are various definitions followed by different authors and in this article we consider some which have survived almost a century as well. In addition, we add our own calculations.

4.1. Active Layer Depth as in [Hill] [3].

Some papers like [Pirt] [6], [Coyte] [2] follow the formula provided by [Hill] [3] assuming that over an extended period of time, the active

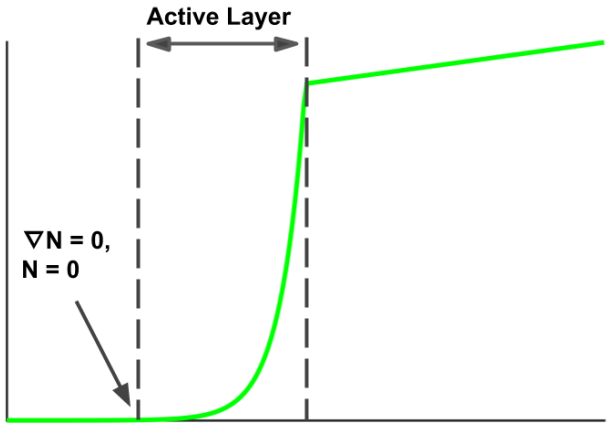

FIGURE 1. Illustration of the active layer depth as in [Hill] [3] (4.1).

layer has a constant depth which may be estimated as

$$|\Omega_a(t)| = \sqrt{\frac{2N_{bd}d_{N,b}}{m(N_{bd})}} \tag{4.1}$$

where $m(N_{bd})$ is used as the maximum uptake rate of the nutrient by the biofilm. This approach gives an underestimate of the active layer depth since the uptake rate is not constant during the simulation period. Formula (4.1) is taken from [Hill] [3], where the derivation assumes that at the active layer depth, $|\Omega_a(t)|$, the nutrient concentration satisfies

$$N(x,t) = 0,\ \nabla N(x,t) = 0\ \forall x \in \partial\Omega_a(t)\backslash\{\gamma\} \tag{4.2}$$

In other words, at the active layer depth the nutrient concentration is 0 and hence diffusion must stop since the concentration cannot become negative. This is illustrated in Fig. 1.

4.2. **Active Layer Depth as in [Dockery, Klapper]** [4]**.** [Dockery, Klapper] [4] have similar formula for the case of an infinite domain

$$|\Omega_a(t)| = \sqrt{\frac{N_{bd}d_{N,b}}{m(N_{bd})}} \tag{4.3}$$

The no flux boundary condition is imposed at $x = -\infty$. In contrast to the boundary conditions imposed by [Hill] [3], the absence of boundary conditions is illustrated in Fig. 2

4.3. **Active Layer Depth as in [McCarty]** [8]**.** A Dirichlet condition on the nutrient concentration N at the active layer depth can further be imposed i.e.

$$N(x,t) = N_*,\ \nabla N(x,t) = 0\ \forall x \in \partial\Omega_a(t)\backslash\{\gamma\} \tag{4.4}$$

for a fixed $N_*([\text{kg/m}^3])$, $N_* > 0$, which allows N to be non-negative in the "inactive layer" $\Omega_b\backslash\Omega_a$. This is illustrated in Fig. 3

Considering the above three definitions, we define the active layer to be the region

$$\Omega_a(t) = \{x < \gamma(t)\ : N(x,t) > N_*\} \tag{4.5}$$

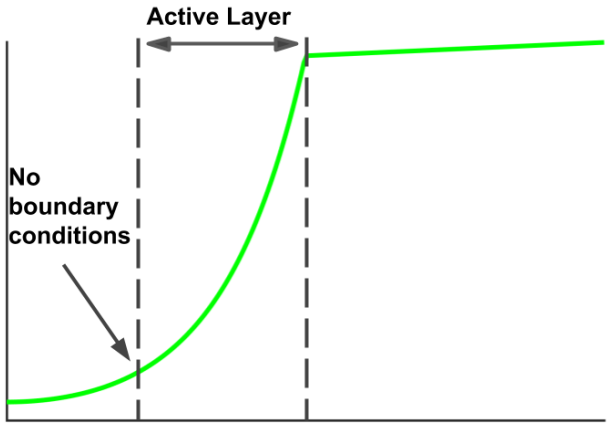

FIGURE 2. Illustration of the active layer depth as in [KD02] [4] (4.2). **Notice** the absence of boundary conditions in determining the active layer depth.

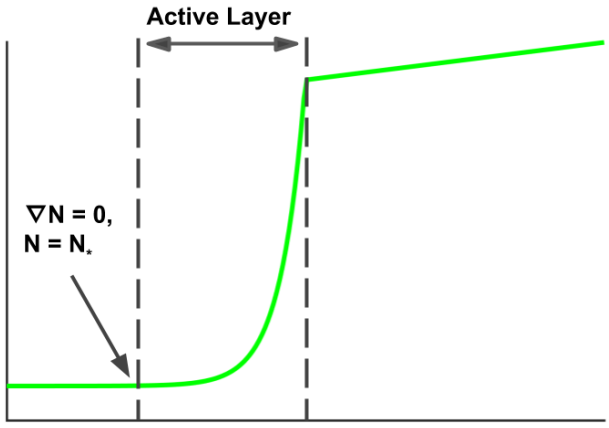

FIGURE 3. Illustration of the active layer depth as in [McCarty] [8] (4.3).

without imposing the no-flux boundary condition as in (4.1) and (4.3). Further, by imposing the no-flux condition at $x = 0$ allows the nutrient concentration to be non-constant in the "inactive layer".

The size of the active layer depth $|\Omega_a|$ is influences the velocity of the biofilm domain Ω_b. Following the reduced model of [KD02], the growth rate of the biofilm domain Ω_b is determined by the rate of change of the interface $\gamma(t)$ i.e. by the velocity of the interface

$$\frac{d\gamma}{dt} = v|_{\gamma(t)} = -\nabla\pi|_{\gamma(t)} \tag{4.6}$$

The dependence of the growth rate on the parameters $N_{bd}, R_{N,bw}, \kappa_b$ is discussed in the subsequent sections. For the linear and constant cases, the active layer depth is explictily calculated as well. Tab . 2 lists the typical values of these parameters.

Parameter	Value
L	$\mathrm{O}(10^{-4})$ [m]
N_{bd}	10^{-3} [kg/m^3]
$d_{N,b}$	1.833×10^{-9} [m^2/s]
$d_{N,w}$	1.66×10^{-9} [m^2/s]
T	$O(0.036 \times 10^5)$ [s]
κ	2×10^{-5} [s^{-1}]
k_N	2×10^{-5} [kg/m^3]
κ_B	0.5

TABLE 2. Typical parameter values

taken from [Alpkvist, Klapper] [1].

Remark. *Henceforth, the* ***numerical active layer depth*** *will refer to the value computed according to* (4.5) *and the* ***analytical active layer depth*** *will be computed using* (4.3).

5. Analytical Solutions to the Stationary Problem

When the expression for the uptake rate m is taken as either of its approximations as given in (2.4), the analytical solutions to the stationary problem (2.5) can be computed and are discussed below.

5.1. **Case 1:** $m(N) = \kappa$**.** The Monod expression can be approximated as $m(N) \approx \kappa$ when $N >> k_N$. In this case, the solution to the stationary problem (2.5) can be calculated and is given by

$$N(x) = \begin{cases} \frac{\kappa}{2d_{N,b}}(x^2 - \gamma^2) + N_\gamma^c & , x \in (0, \gamma) \\ \frac{N_{bd} - N_\gamma^c}{L-\gamma}(x - \gamma) + N_\gamma^c & , x \in (\gamma, L) \end{cases}, \tag{5.1}$$

$$N_\gamma^c = \left(\frac{N_{bd}}{L-\gamma} - \frac{\kappa\gamma}{d_{N,w}}\right)(L - \gamma). \tag{5.2}$$

In this case, the active layer would be

$$\Omega_a(t) = \{x \ : \frac{\kappa}{2d_{N,b}}(x^2 - \gamma^2) + \left(\frac{N_{bd}}{L-\gamma} - \frac{\kappa\gamma}{d_{N,w}}\right)(L - \gamma) > N_*\} \tag{5.3}$$

Note that not all parameter values give physical meaning to (5.1). An important criterion is

$$N(0) = \frac{\kappa}{2d_{N,b}}(-\gamma^2) + N_\gamma^c > 0 \tag{5.4}$$

to ensure that $N > 0$ in Ω_b. Letting $\gamma = \beta L$, for some fraction $\beta > 0$ (typically $\beta \approx \frac{1}{2}$), we get a constraint on the size of the domain L:

$$L < \sqrt{\frac{\frac{N_{bd} d_{N,w}}{\kappa}}{\beta(1 + \beta(\frac{1}{2R_{N,bw}} - 1))}} \tag{5.5}$$

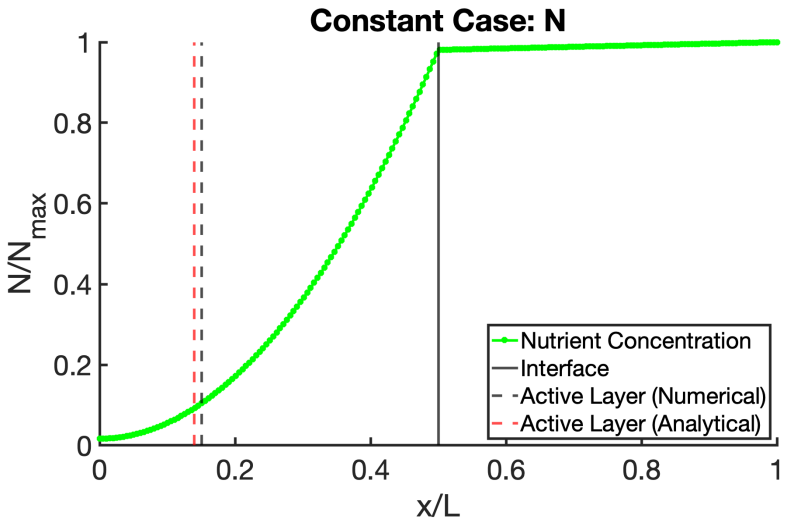

FIGURE 4. Illustration of Ex. 5.1 showing the values of the nutrient concentration N for the constant case. Also shown is the active layer depth (analytical and numerical). The values of the parameters used are $L = 8 \times 10^{-5}$[m], $R_{N,bw} = 0.01$, $N_{bd} = 10^{-3}$[kg/m^3], $\frac{N_*}{N_{bd}} = 0.1$ and the interface is at $\gamma = \frac{L}{2}$.

Example 5.1. *Using the parameters listed in Tab. 2, we plot the solution given in* (5.1) *in Fig. 4. Also shown is the interface, the analytical* (4.3) *and the numerical* (4.5) *active layer depths.*

Example 5.2. *Using the parameters listed in Tab. 2, we plot the computed numerical (*(4.5)*) and analytical (*(4.3)*) values of the active depth layer as a function of $R_{N,bw}$ using equation* (5.1) *in Fig. 5.*

Example 5.3. *Using the parameters listed in Tab. 2, we plot the showing the computed numerical (*(4.5)*) and analytical (*(4.3)*) values of the active depth layer as a function of N_{bd} using equation* (5.1) *in Fig. 6.*

From the above examples, when m is constant, the following observations are made about the active layer depth $|\Omega_a|$.

(1) $|\Omega_a|$ increases with increasing $R_{N,bw}$. This increase is expected since increasing $R_{N,bw}$ increases the flux $d_{N,b}\nabla N|_{x=\gamma}$ leading to more nutrient diffusion across the interface and increasing the biofilm growth.
(2) $|\Omega_a|$ increases with increasing N_{bd}. This increase is expected as well since a higher nutrient concentration leads to more diffusion across the interface which leads to an increase in the biofilm growth.

5.2. **Case 2:** $m(N) = \frac{\kappa}{k_N}N$**.** In the case when $N << k_N$, the Monod expression can be approximated as $m(N) \approx \frac{\kappa}{k_N}N$. The solution to the stationary problem (2.5) can be

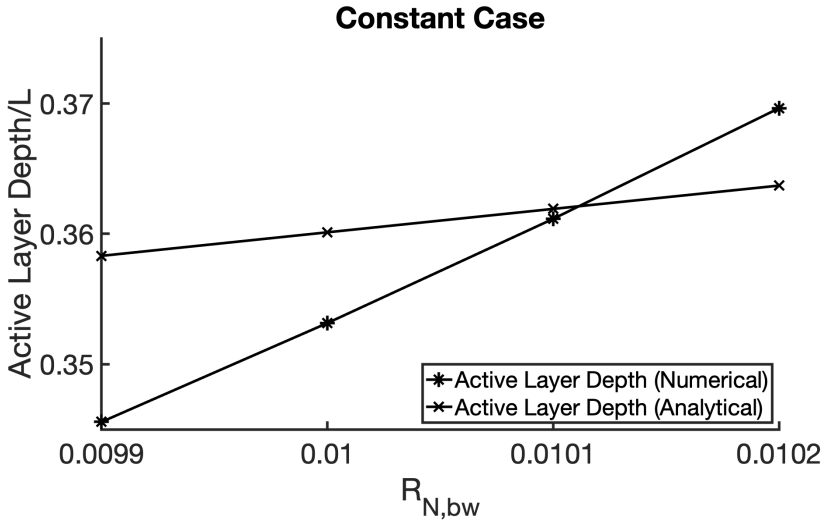

FIGURE 5. Illustration of Ex. 5.2 showing the values of the active layer depth for the linear case as a function of $R_{N,bw}$. The values of the parameters used are $L = 8 \times 10^{-5}$[m], $N_{bd} = 10^{-3}$[kg/m^3], $\frac{N_*}{N_{bd}} = 0.1$ and the interface is at $\gamma = \frac{L}{2}$.

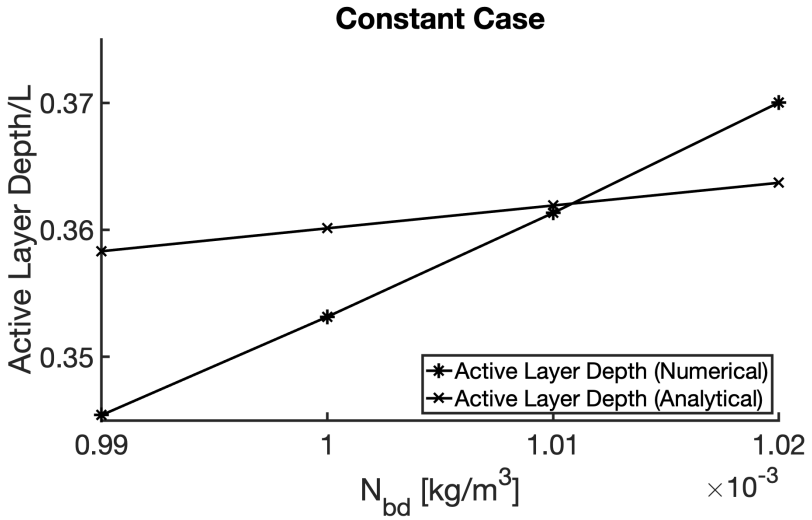

FIGURE 6. Illustration of Ex. 5.3 showing the values of the active layer depth for the linear case as a function of $R_{N,bw}$. The values of the parameters used are $L = 8 \times 10^{-5}$[m], $R_{N,bw} = 0.01$, $\frac{N_*}{N_{bd}} = 0.1$ and the interface is at $\gamma = \frac{L}{2}$.

calculated, and is given by

$$N(x) = \begin{cases} \frac{N_\gamma^l}{e^{\rho\gamma}+e^{-\rho\gamma}}(e^{\rho x}+e^{-\rho x}) & , x \in (0,\gamma) \\ (\frac{N_{bd}-N_\gamma^l}{L-\gamma})(x-\gamma)+N_\gamma^l & , x \in (\gamma, L) \end{cases}, \tag{5.6}$$

$$N_\gamma^l = \left(\frac{N_{bd}}{L-\gamma}\right)\left(R_{N,bw}\rho\tanh(\rho\gamma)+\frac{1}{L-\gamma}\right)^{-1}, \tag{5.7}$$

$$\rho = \sqrt{\frac{\kappa}{d_{N,b}k_N}} = \frac{1}{\sqrt{\frac{N_{bd}d_{N,b}}{m(N_{bd})}}} = \sqrt{\frac{\kappa}{R_{N,bw}d_{N,w}k_N}}. \tag{5.8}$$

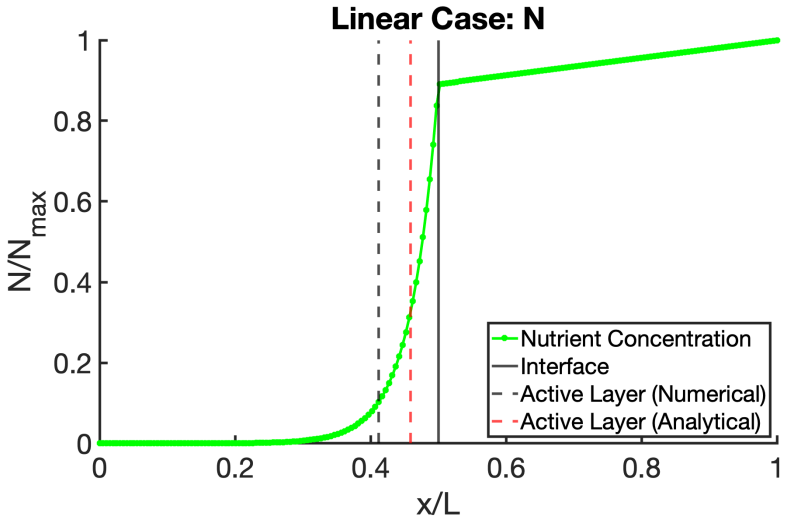

FIGURE 7. Illustration of Ex. 5.4 showing the values of the nutrient concentration N for the linear case. Also shown is the active layer depth (analytical and numerical). The values of the parameters used are $L = 1 \times 10^{-4}$[m], $R_{N,bw} = 0.01$, $N_{bd} = 10^{-7}$[kg/m^3], $\frac{N_*}{N_{bd}} = 0.1$ and the interface is at $\gamma = \frac{L}{2}$.

Remark. *The expression for ρ justifies the analytical active layer formula given by [Dockery, Klapper] [4] in (4.3): the width of the region where $N \sim O(1)$ is $\frac{1}{\rho}$.*

Based on these calculations we now get that the active layer is

$$\Omega_a(t) = \{x : e^{\rho x} + e^{-\rho x} > \frac{N_*}{N_{bd}} \ ((L-\gamma)R_{N,bw}\rho \tanh \rho\gamma + 1)\,(e^{\rho\gamma} + e^{-\rho\gamma})\} \tag{5.9}$$

Example 5.4. *Using the parameters listed in Tab. 2, we plot the solution given in (5.6) in Fig. 7. Also shown is the interface, the analytical (4.3) and the numerical (4.5) active layer depths.*

Example 5.5. *Using the parameters listed in Tab. 2, we plot the computed numerical ((4.5)) and analytical ((4.3)) values of the active depth layer as a function of $R_{N,bw}$ using equation (5.6) in Fig. 8.*

Example 5.6. *Using the parameters listed in Tab. 2, we plot the computed numerical ((4.5)) and analytical ((4.3)) values of the active depth layer as a function of N_{bd} using equation (5.6) in Fig. 9.*

Remark. *In this example, the value of N_* is fixed to 10^{-8}[kg/m^3] instead of taking it as a fraction of N_{bd}. This is because if $\frac{N_*}{N_{bd}} = const$, then the numerical active layer depth (4.5) would be a constant as can be seen in (5.9).*

Based on the above examples, when m is linear, similar observations can be made about the active layer depth $|\Omega_a|$.

(1) $|\Omega_a|$ increases with increasing $R_{N,bw}$. As in the constant case, this increase is expected since increasing $R_{N,bw}$ increases the flux $d_{N,b}\nabla N|_{x=\gamma}$ leading to more nutrient diffusion across the interface and increasing the biofilm growth.

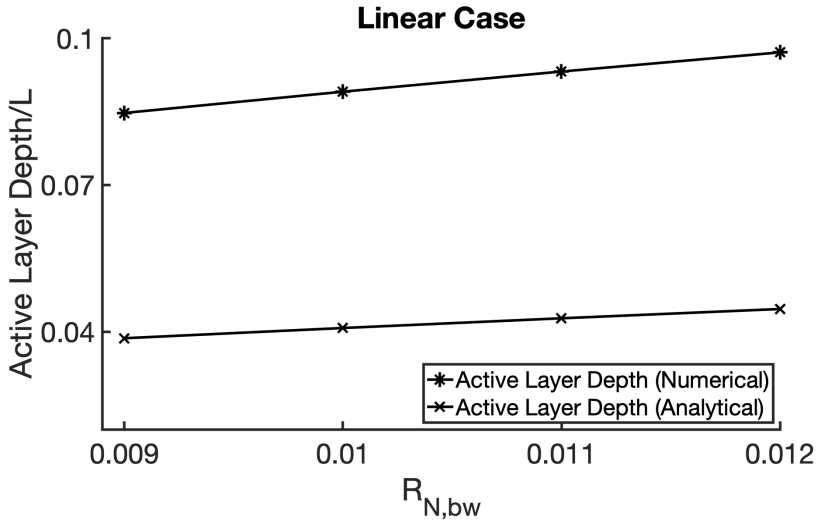

FIGURE 8. Illustration of Ex. 5.5 showing the values of the active layer depth for the linear case as a function of $R_{N,bw}$. The values of the parameters used are $L = 1 \times 10^{-4}$[m], $N_{bd} = 10^{-7}$[kg/m^3], $\frac{N_*}{N_{bd}} = 0.1$ and the interface is at $\gamma = \frac{L}{2}$.

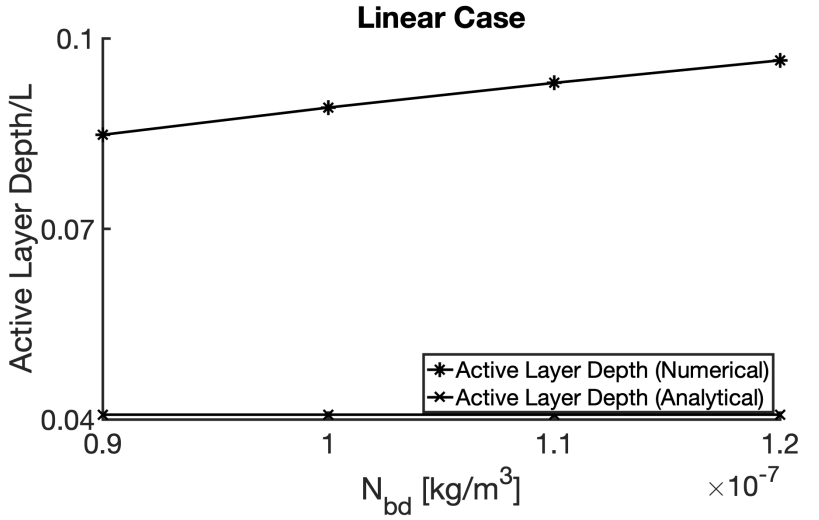

FIGURE 9. Illustration of Ex. 5.6 showing the values of the active layer depth for the linear case as a function of N_{bd}. The values of the parameters used are $L = 1 \times 10^{-4}$[m], $R_{N,bw} = 0.01$, $N_* = 1 \times 10^{-8}$[kg/m^3] and the interface is at $\gamma = \frac{L}{2}$.

(2) $|\Omega_a|$ increases with increasing N_{bd}. This increase is also expected since a higher nutrient concentration leads to more diffusion across the interface which leads to an increase in the biofilm growth.

Active Layer Depth Comparison. Though the active layer depth $|\Omega_a|$ follows the same behaviour for the constant and linear case, there are still a few subtleties that are observed.

(1) The depth $|\Omega_a|$ increases with increasing $R_{N,bw}$ but is more "sensitive" to parameter variation in the constant case than in the linear case.
(2) The depth $|\Omega_a|$ increases with increasing N_{bd} but as in the case with $R_{N,bw}$, the constant case is more "sensitive" to small perturbations in N_{bd} than the linear case. Also, in the linear case, the **analytical active layer depth** is independent of N_{bd} and stays constant.

6. Interface Velocity

The growth of the biofilm drives the interface γ. In this section, we study the velocity of the interface $v|_\gamma$ and its relation to the active layer depth $|\Omega_a|$. Further, we also study the dependence of the velocity on the parameters used in Tab. 2.

6.1. **Interface Velocity and the Active Layer Depth.** For the linear case (5.6) with an infinite domain, [Dockery, Klapper] [4] derive a constant interface velocity which leads to a linear growth of the interface. This constant growth rate is a result of an invariance in the nutrient concentration because of the infinite domain and is simply the active layer depth multiplied with the biofilm growth function at the interface: consider the stationary biofilm-nutrient model for the infinite domain

$$-\nabla(d_N(x)\nabla N) = -\chi_{(-\infty,\gamma)}m(N) \text{ in } (-\infty, L) \tag{6.1a}$$
$$\nabla N|_{x=-\infty} = 0,\ N(L,t) = N_{bd} \tag{6.1b}$$
$$\nabla \cdot v = g(N),\ v = -\nabla\pi \text{ in } (-\infty, L) \tag{6.1c}$$
$$\nabla\pi|_{x=-\infty} = 0,\ \pi|_{x=\gamma} = 0. \tag{6.1d}$$

with $d_N(x) = d_{N,b}\chi_{(-\infty,\gamma)} + d_{N,w}\chi_{(\gamma,L)}$. For the specific case, as in [4], when $m(N) = \frac{\kappa}{k_N}N$ and $g(N) = \kappa_B m(N)$, the solution to the above system (6.1) is given by

$$N(x) = \begin{cases} \frac{N_\gamma^l}{e^{\rho\gamma}}e^{\rho x} & ,\ x \in (\infty, \gamma) \\ (\frac{N_{bd}-N_\gamma^l}{L-\gamma})(x-\gamma) + N_\gamma^l & ,\ x \in (\gamma, L) \end{cases}, \tag{6.2}$$

$$N_\gamma^l = \left(\frac{N_{bd}}{L-\gamma}\right)\left(R_{N,bw}\rho + \frac{1}{L-\gamma}\right)^{-1}, \tag{6.3}$$

where

$$\rho = \sqrt{\frac{\kappa}{d_{N,b}k_N}} = \frac{1}{\sqrt{\frac{N_{bd}d_{N,b}}{m(N_{bd})}}} = \frac{1}{|\Omega_a|} = \sqrt{\frac{\kappa}{R_{N,bw}d_{N,w}k_N}}. \tag{6.4}$$

Using the definition of the active layer depth (4.3) ($|\Omega_a| = \frac{1}{\rho}$), the interface velocity can be written as

$$v|_\gamma = \int_{-\infty}^{\gamma} -\nabla^2\pi = \int_{-\infty}^{\gamma} g(m(N)) = \int_{-\infty}^{\gamma} \kappa_B\frac{\kappa}{k_N}N = \left(\frac{\kappa_B\kappa}{k_N}\right)\frac{N_\gamma^l}{\rho} = \frac{1}{\rho}\kappa_B\left(\frac{\kappa N_\gamma^l}{k_N}\right) \tag{6.5a}$$
$$= \frac{1}{\rho}g(m(N_\gamma^l)) = |\Omega_a|g(N_\gamma^l) \tag{6.5b}$$

i.e. the velocity is the product of the active layer depth and the growth rate at the interface and is a **constant** if either the growth rate g or N_γ^l is a constant. In [4], $L = \gamma + l$, for a constant $l > 0$, which leads to a constant N_γ^l.

Now consider the stationary system (6.2) for a finite domain i.e. consider the system

$$-\nabla(d_N(x)\nabla N) = -\chi_{(0,\gamma)}m(N) \text{ in } (0,L) \tag{6.6a}$$

$$\nabla N|_{x=0} = 0,\ N(L,t) = N_{bd} \tag{6.6b}$$

$$\nabla \cdot v = g(N),\ v = -\nabla\pi \text{ in } (0,L) \tag{6.6c}$$

$$\nabla\pi|_{x=0} = 0,\ \pi|_{x=\gamma} = 0. \tag{6.6d}$$

When $m = \kappa$ and $g = \kappa_B m$ the solution to the above system (6.6) is given by (5.1). In this case, the velocity of the interface is

$$v|_\gamma = \int_{-\infty}^{\gamma} \kappa_B\kappa = (\kappa_B\kappa)\,\gamma = \gamma\,(\kappa_B\kappa) = \gamma g(N_\gamma^c). \tag{6.7}$$

We note that in this case, the velocity of the interface is not a constant (since $\gamma \equiv \gamma(t)$ is not constant). If the velocity in (6.7) is to be viewed as the product of the active layer depth and the growth rate at the interface, then the active layer depth would have to be defined as

$$|\Omega_a(t)| = \gamma \tag{6.8}$$

However, when $m = \frac{\kappa}{k_N}N$ and $g = \kappa_B m$ the solution to the above system (6.6) is given by (5.6) and in this case the velocity of the interface is

$$v|_\gamma = \int_{-\infty}^{\gamma} \kappa_B \frac{\kappa}{k_N} N = \left(\frac{\kappa_B\kappa}{k_N}\right)\frac{N_\gamma^l \tanh(\rho\gamma)}{\rho} = \left(\frac{\tanh(\rho\gamma)}{\rho}\right)\kappa_B\left(\frac{\kappa N_\gamma^l}{k_N}\right) \tag{6.9a}$$

$$= \left(\frac{\tanh(\rho\gamma)}{\rho}\right) g(m(N_\gamma^l)) = \tanh(\rho\gamma)|\Omega_a| g(N_\gamma^l). \tag{6.9b}$$

Similar to the constant case (6.7), the velocity of the interface is not constant. Again, if the velocity (6.9)is to be interpreted as the product of the active layer depth and the growth rate at the interface, then the active layer depth would have to be defined as

$$|\Omega_a(t)| = \frac{\tanh(\rho\gamma)}{\rho}. \tag{6.10}$$

Motivated by the above formulation, we now compare the velocity of the interface $v|_\gamma$ and the product of the numerical active layer depth (4.5) and the growth rate at the interface for the **non-stationary** model (2.1a).

Example 6.1. *We plot the time-averaged values of the velocity $v|_\gamma$ and the product of the active layer depth $|\Omega_a|$ and the growth rate at the interface $g(N_\gamma)$, where N_γ is the nutrient concentration at the interface γ, in Fig. 10. The two values are computed as a function of the boundary value N_{bd}.*

Example 6.2. *We plot the time-averaged values of the velocity $v|_\gamma$ and the product of the active layer depth $|\Omega_a|$ and the growth rate at the interface $g(N_\gamma)$, where N_γ is the nutrient concentration at the interface γ, in Fig. 11. The two values are computed as a function of the ratio $R_{N,bw}$.*

The above two examples 6.1 and 6.2 show a strong correlation between the velocity of the interface $v|_\gamma$ and the product of the active layer depth $|\Omega_a|$ and the growth rate at the interface $g(N_\gamma)$. Though there is a difference in the magnitude of the values but that is to

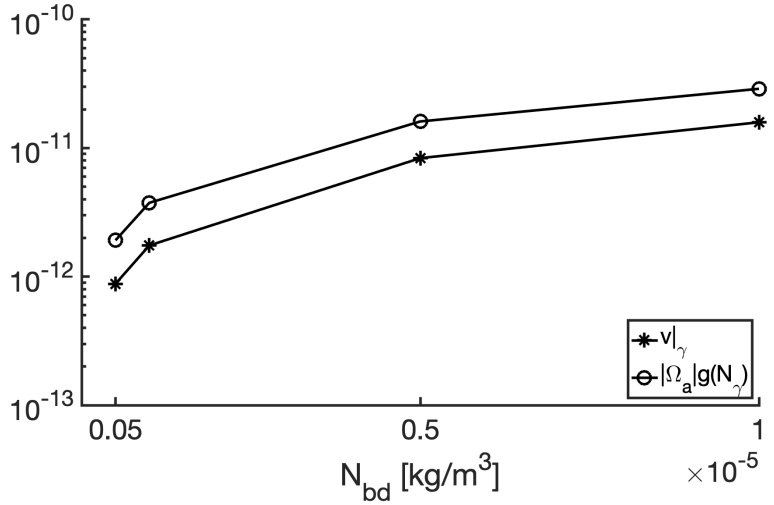

FIGURE 10. Illustration of Ex. 6.1 showing the time-averaged velocity of the biofilm interface v_γ and the time-averaged value of the product $|\,\Omega_a\,| \times g(N_\gamma)$ as N_{bd} varies. The values of the parameters used are $L = 1\times10^{-4}$[m], $R_{N,bw} = 0.01$, $\frac{N_*}{N_{bd}} = 0.1$ and the interface is at $\gamma = \frac{L}{2}$.

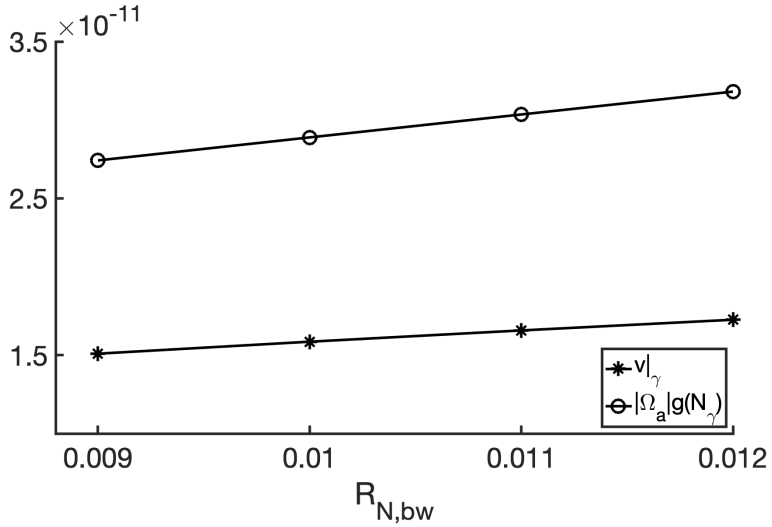

FIGURE 11. Illustration of Ex. 6.2 showing the time-averaged velocity of the biofilm interface v_γ and the time-averaged value of the product $|\,\Omega_a\,| \times g(N_\gamma)$ as $R_{N,bw}$ varies. The values of the parameters used are $L = 1 \times 10^{-4}$[m], $N_{bd} = 1 \times 10^{-5}$[kg/m^3], $\frac{N_*}{N_{bd}} = 0.1$ and the interface is at $\gamma = \frac{L}{2}$.

be expected since the numerical active layer depth (4.5) depends on an a priori constant N_*. This difference can be minimised, however, by adjusting the value of N_* accordingly.

6.2. **Interface Velocity and Parameter Dependence.** The interface velocity $v|_\gamma$ also depends on the different parameters that are used, namely $\kappa_B, N_{bd}, R_{N,bw}$. This dependence is explored in the examples below.

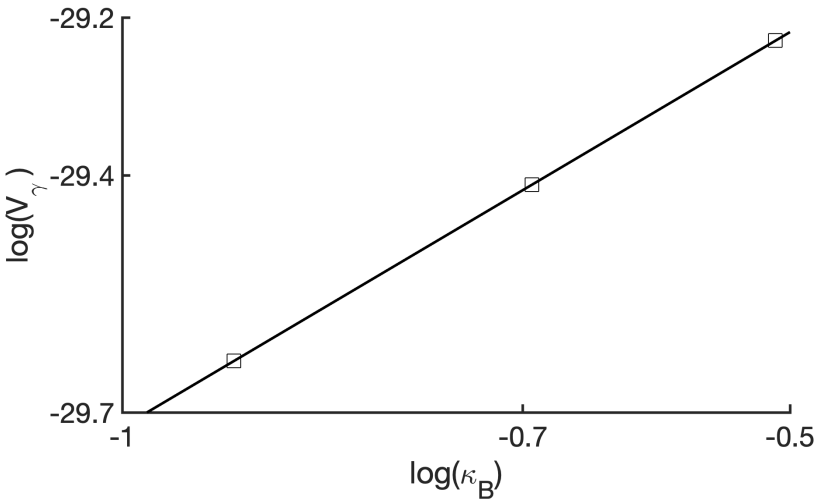

FIGURE 12. Illustration of Ex. 6.3 showing the relation between the velocity of the biofilm interface γ and κ_B (the velocity has been non-dimensionalised by dividing it with a factor of 1[m/s]). The values of the parameters used are $L = 1 \times 10^{-5}$[m], $R_{N,bw} = 0.01$, $N_{bd} = 1 \times 10^{-7}$[kg/m^3], $\frac{N_*}{N_{bd}} = 0.1$ and the interface is at $\gamma = \frac{L}{2}$. Also shown is the linear fit with a slope of 1.00007.

Example 6.3. *The dependence of the time-averaged velocity of the interface $v|_\gamma$ on κ_B is shown in Fig. 12. The increase is as expected since the parameter κ_B incorporates the yield coefficient and the maximum uptake rate. The slope of the linear fit, ≈ 1, is because of the direct dependence of v on κ_B*

$$\nabla \cdot v = \kappa_B \frac{\kappa N}{k_N + N} \tag{6.11}$$

Example 6.4. *The dependence of the time-averaged velocity of the interface $v|_\gamma$ on the Dirichlet value N_{bd} is shown in Fig. 13. The increase is expected since a greater nutrient concentration increases the rate of the biofilm growth and hence the velocity of the interface.*

Example 6.5. *The dependence of the time-averaged velocity of the interface $v|_\gamma$ on the ration $R_{N,bw}$ is shown in Fig. 14. The increase is expected since $R_{N,bw} = \frac{d_{N,b}}{d_{N,w}}$ and an increase in $R_{N,bw}$ implies an increase in $d_{N,b}$, thereby increasing the flux $d_{N,b}\nabla N$ which leads to more diffusion of the nutrient across the interface and hence increases the growth rate of the biofilm.*

Summary. Based on the above three examples, we make the following observations about the velocity $\frac{d\gamma}{dt} = v|_{x=\gamma}$ of the interface.

(1) $v|_{x=\gamma}$ increases linearly with κ_B.
(2) $v|_{x=\gamma}$ increases with increasing nutrient concentration N_{bd}.
(3) $v|_{x=\gamma}$ increases with increasing $R_{N,bw}$.

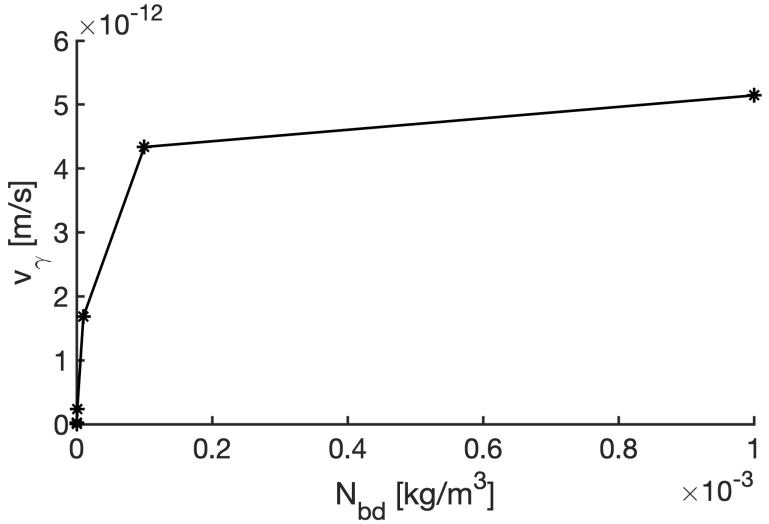

FIGURE 13. Illustration of Ex. 6.4 showing the relation between the velocity of the biofilm interface γ and N_{bd}. The values of the parameters used are $L = 1 \times 10^{-6}$[m], $R_{N,bw} = 0.01$, $\frac{N_*}{N_{bd}} = 0.1$ and the interface is at $\gamma = \frac{L}{2}$.

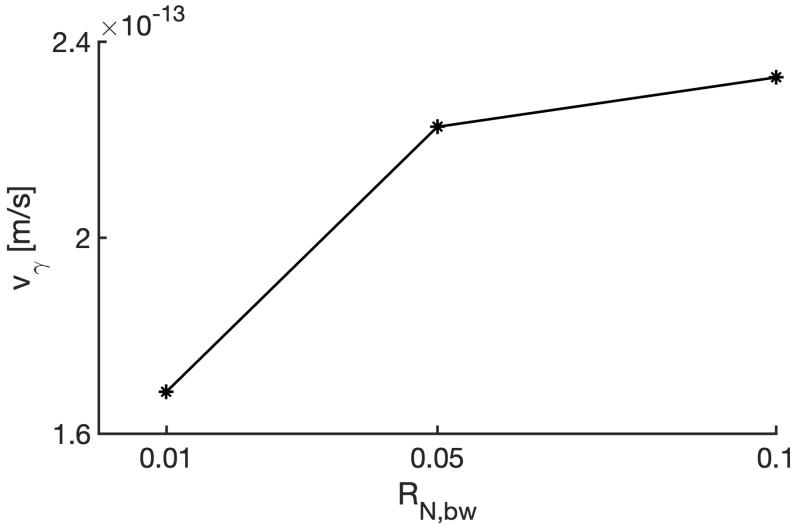

FIGURE 14. Illustration of Ex. 6.5 showing the relation between the velocity of the biofilm interface γ and N_{bd}. The values of the parameters used are $L = 1 \times 10^{-5}$[m], $R_{N,bw} = 0.01$, $N_{bd} = 1 \times 10^{-7}$[kg/m^3], $\frac{N_*}{N_{bd}} = 0.1$ and the interface is at $\gamma = \frac{L}{2}$.

7. Error Analysis

The above sections deal with the linear and constant cases of the stationary problem (2.5) and depending on the magnitude of the ratio $\frac{k_N}{N_{bd}}$, the analytical solutions (5.1) and (5.6) provide an approximation to the original non-stationary problem (2.1a). Hence, for particular values of the parameters, namely k_N, N_{bd} and L, the non-stationary solution would follow

L[m]	N_{bd} [kg/m^3]	k_N[kg/m^3]	$\frac{k_N}{N_{bd}}$	% Error L^2Linear	% Error L^2Constant
1×10^{-3}	10^{-8}	2×10^{-5}	2×10^{3}	28.2037	–
1×10^{-4}	10^{-8}	2×10^{-5}	2×10^{3}	8.1641	–
1×10^{-5}	10^{-8}	2×10^{-5}	2×10^{3}	1.271	–
1×10^{-6}	10^{-8}	2×10^{-5}	2×10^{3}	2.7×10^{-3}	–
1×10^{-3}	10^{-6}	2×10^{-5}	2×10^{1}	28.2662	–
1×10^{-4}	10^{-6}	2×10^{-5}	2×10^{1}	8.286	–
1×10^{-5}	10^{-6}	2×10^{-5}	2×10^{1}	1.9426	–
1×10^{-6}	10^{-6}	2×10^{-5}	2×10^{1}	2.8814×10^{-2}	10.8792
1×10^{-5}	10^{-4}	2×10^{-5}	2×10^{-1}	28.9346	2.6403
1×10^{-6}	10^{-4}	2×10^{-5}	2×10^{-1}	5.8037×10^{-1}	2.3885×10^{-2}

TABLE 3. Error values between the stationary approximation and the non-stationary solution as discussed in Sec. 7. The symbol " $-$ " marks the cases where the nutrient concentration takes negative values.

the same behaviour as the stationary solution, which is easier to study owing to the existence of its analytical expression.

In this section, the aforementioned approximation is quantified by calculating the $L^\infty((0,T),L^2(0,L))$ error

$$\text{Relative Error } (\%) = \frac{\|N_s - N_{ns}\|_{L^\infty((0,T),L^2(0,L))}}{\|N_{ns}\|_{L^\infty((0,T),L^2(0,L))}} \times 100, \tag{7.1}$$

where N_{ns} is the solution to the non-stationary problem (2.1a) and N_s is the solution to the stationary problem (2.5) with uptake rate as given by (5.1) or (5.6), referred to as the constant and the linear case, respectively.

We simulate the non-stationary and stationary cases and calculate the error for different choices of the size L of the domain ($L \in [1, 1000][\mu\text{m}]$) and of the Dirichlet boundary value N_{bd}; see Tab. 3.

The data in Tab. 3 supports the following observations:

(1) For a fixed L, as the ratio $\frac{k_N}{N_{bd}}$ decreases, the non-stationary system is better approximated by the constant case than the linear case as is reflected by the relative error.
(2) When fixing $\frac{k_N}{N_{bd}}$ and decreasing L, the relative error decreases. Mathematically, this can be proved by non-dimensionalising the non-stationary system (2.1a).

Remark. *For certain cases, the analytical solution to the stationary problem with constant m as in* (5.1) *violates condition* (5.5) *thereby leading to N_s taking negative values. Such cases are marked by a " $-$ " in Tab. 3.*

8. SUMMARY

In this article, we primarily explored the growth aspect of the biofilm-nutrient model. We started by exploring the various definitions of the active layer depth $|\Omega_a|$ and its dependence on the different parameters used in the biofilm-nutrient model. Then, we also computed

the active layer depth for the analytical solutions to the stationary problem (2.5) to get a comparison between these different definitions.

Next, we studied the dependence of the velocity of the interface on the boundary value N_{bd} and the ratio $R_{N,bw}$. Further, some manipulation allowed us to analyse the role of the active layer depth in the velocity of the interface, and this role was then explored for the original non-stationary system (2.1a).

Finally, since we used the analytical solutions to the stationary problem as an approximation to the non-stationary system, we quantified the error of this approximation to validate our analysis.

9. Acknowledgement

The work presented was undertaken under the guidance of Professor Malgorzata Peszynska and was completed in Fall 2020. The analysis was performed as a part of the paper [7], the manuscript of which has been submitted.

References

[1] E. Alpkvist and I. Klapper, A multidimensional multispecies continuum model for heterogeneous biofilm development, *Bulletin of mathematical biology*, **69** (2007), 765–789.

[2] K. Z. Coyte, H. Tabuteau, E. A. Gaffney, K. R. Foster and W. M. Durham, Microbial competition in porous environments can select against rapid biofilm growth, *Proceedings of the National Academy of Sciences - PNAS*, **114** (2017), E161–E170.

[3] A. V. Hill, The diffusion of oxygen and lactic acid through tissues, *Proceedings of the Royal Society B*, **104**.

[4] I. Klapper and J. Dockery, Finger formation in biofilm layers, *SIAM journal on applied mathematics*, **62** (2002), 853–869.

[5] R. J. LeVeque, Finite difference methods for ordinary and partial differential equations: Steady-state and time-dependent problems.

[6] S. Pirt, A kinetic study of the mode of growth of surface colonies of bacteria and fungi, *Microbiology*, **47** (1967), 181–197.

[7] C. Shin, A. Alhammali, L. Bigler, N. Vohra and M. Peszynska, Coupled flow and biomass-nutrient growth at pore-scale with permeable biofilm, adaptive singularity and multiple species, *Manuscript submitted.*

[8] K. Williamson and P. L. McCarty, A model of substrate utilisation by bacterial films, *Journal (Water Pollution Control Federation)*, **48** (1976), 9–24.